Journal of Applied Polymer Science

Flame retardancy and thermal and mechanical performance of intercalated, layered double hydroxide composites of polyamide 11, aluminum phosphinate, and sulfamic acid

Sheng Zhang,[1] Wufei Tang,[1] Xiaoyu Gu,[1] Peng Jiang,[1] Jun Sun,[1] Duquesne Sophie,[2] Serge Bourbigot,[2] Mathilde Casetta[2]

[1]Key Laboratory of Carbon Fiber and Functional Polymers (Beijing University of Chemical Technology, Ministry of Education), Beijing 100029, China

[2]ENSCLISP-UMET, F-59652, Villeneuve d'Ascq, France

Correspondence to: X. Gu (E-mail: guxy@mail.buct.edu.cn)

ABSTRACT: Sulfamic acid-intercalated MgAl-layered double hydroxide (SA-LDH) was prepared and added with aluminum phosphinate (AlPi) into polyamide 11 (PA11). The results showed that AlPi/SA-LDH made a positive contribution to both flame retardancy and thermostability, and the effect was demonstrated with the limiting oxygen index (LOI), vertical burning tests (UL-94), cone calorimetry (CONE), and thermogravimetric analysis (TGA). The char morphologies were observed by SEM, and its chemical composition was investigated by Fourier transform infrared spectroscopy (FTIR). The decomposition mechanism was examined by TGA-FTIR. The results showed that the LOI of PA11 was only 23.0 and cannot pass any UL-94 rating. The addition of 20% AlPi increased the LOI to 31.5 and passed the UL-94 V-1 rating, and AlPi/SA-LDH 15%/5% increased the LOI to 32.4 and also passed the UL-94 V-1 rating. The CONE results revealed that 20% of either AlPi or AlPi/SA-LDH brought about a 30% decrease in the peak heat release rate (pHRR). The contribution of SA-LDH to flame behavior was especially reflected in the postponement of pHRR. SEM showed that the char morphologies became denser after SA-LDH incorporation. The improvement in thermal stability of the AlPi/SA-LDH combination was documented by TGA in both N_2 and air atmospheres. The mechanical performance deterioration caused by AlPi was partly improved by SA-LDH. The storage modulus (E') below the T_g of AlPi/SA-LDH 15%/5% was about 300 MPa higher than with 20% AlPi. This was attributed to a compatibility improvement. The interaction forces among PA11, AlPi, and SA-LDH were probed by X-ray photoelectron spectrometry. © 2016 Wiley Periodicals, Inc. J. Appl. Polym. Sci. **2016**, *133*, 43370.

KEYWORDS: flame retardance; mechanical properties; polyamides; thermogravimetric analysis

Received 8 July 2015; accepted 16 December 2015

DOI: 10.1002/app.43370

INTRODUCTION

Polyamides (PA) are widely used as engineering materials because of their higher tensile and impact strength, stronger abrasive resistance, excellent oil resistivity, and lower moisture absorption.[1] Standing out from all kinds of PA, polyamide 11 (PA11) exhibits superior toughness at low temperature, which is a substantial criteria for certain applications like clinical equipment. Furthermore, PA11 is biomass-based with its monomer (11-amino-undecanoic acid) obtained from castor oil, so more and more attention has been focused on PA11 to reduce the consumption of petroleum.[2]

However, PA is easily flammable according to its basic chemical composition.[3] Among several ways to reduce the fire hazards of polymers, the most popular one is still the incorporation of flame retardants (FR) into the polymer matrix; it is simple and cheap, and numerous FR are commercially available.[4–6] A series of organophosphorus-based FR developed by Clariant with the trade name of Exolit OP have been demonstrated to be effective for PA materials.[7,8] About 15–20% Exolit OP1311 in PA6 yields a UL94 V-0 rating. Ideally, in order to minimize a loss in mechanical properties, flame-retardant concentrations should be below 30 wt %, and the Exolit OP products fulfill this requirement.[9]

Layered double hydroxide (LDH)s can offer good flame retardancy and smoke suppression not only because of their unique chemical composition similar to aluminium hydroxide/magnesium hydroxide (ATH/MH), but also because of their flake-like morphological structure like montmorillonite (MMT).[10–13] Furthermore, some modified LDHs with intercalated flame-retardant anions such as NO_3^- and PO_4^{3-} enhance its flame retardancy.[14,15] Sulfamic acid (SA) and its derivatives have been

Table I. LOI and UL-94 Results for PA11 and Its Composites

PA11/AlPi/SA-LDH	LOI	UL-94
100/0/0	23.0 ± 0.2	No rating
80/20/0	31.5 ± 0.3 (↑6.6)	V-1
80/17.5/2.5	32.1 ± 0.2 (↑7.2)	V-1
80/15/5	32.4 ± 0.1 (↑7.5)	V-1

documented for their flame retardancy in polymers,[16,17] and the synergistic flame retardancy of SA/MMT in PA6 has been reported by Lewin.[18,19]

In this work, a novel sulfamic acid–intercalated MgAl-LDH (SA-LDH) was prepared. SA-LDH was combined with aluminum phosphinate (AlPi) to improve the flame retardancy, thermal stability, and mechanical performance of PA11. The results showed that the AlPi/SA-LDH combination improved the flame retardancy, thermal stability, and mechanical performance compared with only the addition of AlPi.

EXPERIMENTAL

Materials

Polyamide 11 (LOT 142170-75) was provided by Arkema (Serquigny, France). Diethyl aluminum phosphinate (AlPi) with the trade name of Exolit OP1230 (23 wt % phosphorus) was provided by Clariant (Shanghai, China). MgAl-CO_3^{2-} LDH was offered from Nan Tong Advance Chemicals, Nantong, China. Sulfamic acid was provided by Xi Long Chemicals, Shantou, China.

Preparation of SA-LDH

First, 10 g MgAl-CO_3^{2-} LDH was dispersed in 200 mL of deionized water in a 500-mL three-necked distilling flask with vigorous stirring, and then a solution of 10 g SA in 50 mL deionized water was added into this slurry, and the mixture was stirred for 2 h at 50 °C. Finally, the precipitate was washed, filtered, and dried at 60 °C for 24 h. The product was labeled as sulfamic acid–intercalated LDH (SA-LDH).

Preparation of Composites

The PA11/AlPi/SA-LDH composites were melt-compounded on a Thermo Scientific HAAKE Rheomix OS PTW (Waltham, MA), which included a corotating two-screw extruder (barrel length 400 mm and screw diameter $L/D = 25$) equipped with feed-dosing elements. The temperature settings of the 10 zones in the extruder from the hopper to die were 250, 245, 230, 230, 220, 185, 180, 170, 170, and 170 °C, and the screw speed was 65 rpm. The extrudate was pelletized and dried for 14 h at 80 °C before being molded to the suitable size by special injection molders for the limited oxygen index (LOI) and UL-94 vertical burning tests. At the same time, a small sample was ground to a powder in liquid nitrogen in an ultracentrifuge mill for thermogravimetric analysis.

Characterization

Thermogravimetric analysis (TGA) was performed on a TAQ-5000 (TA Instruments, New Castle, Pennsylvania) with a heating rate of 10 °C/min in the range 50–800 °C under both nitrogen and air atmosphere with a gas flow rate of 50 mL/min. The mass of each sample was 3 to 5 mg.

TGA was also coupled with a Nicolet (Waltham, Massachusetts) IS10 Fourier transform infrared (FTIR) spectrometer. The gaseous degradation products from TGA at different temperatures were transferred to the gas cell in the FTIR, and the corresponding spectra were collected.

The FTIR spectra were collected from a Nicolet Nexus 670 FTIR under a resolution of 1 cm^{-1} in 128 scans using KBr pellets.

The LOI was measured according to the ISO1210:1992 standard on a JF-3 oxygen index apparatus (Jiangning, China). The sample dimensions were 100 × 6.5 × 3 mm^3.

The UL-94 vertical burning tests were performed on a CZF-3 apparatus (Jiangning, China) according to ASTM D3801-1996. The sample dimensions were 125 × 12.5 × 3 mm^3.

The X-ray photoelectron spectra (XPS) were recorded with a VG ESCALAB 250 (Thermo Fisher Scientific) using Al Kα excitation radiation ($hv = 1486.6$ eV) and calibrated by assuming the binding energy of carbonaceous carbon to be 284.8 eV.

A cone calorimeter was used to evaluate the fire performance of the composites according to the standard ISO 5660 under a heat flux of 50 kW/m^2 with a size of 100 × 100 × 3 mm^3, which is comparable to that of a mild fire scenario. The specimens were wrapped in aluminum foil, leaving the upper surface exposed to the radiator, and then placed on a ceramic backing board at a distance of 25 mm from the cone base. The experiments were repeated five times.

SEM observation was conducted by means of a field-emission scanning electron microscope Hitachi S-4700(Minneapolis, Minnesota) under the voltage of 20 kV. With each sample fractured in liquid nitrogen and covered with Pt, more than eight SEM images were taken at different magnifications to assess the true morphology.

Dynamic thermomechanical analysis (DMA) was performed on a Remetric Scientific DMTA V (Piscataway, New Jersey) at a frequency of 1 Hz and a heating rate of 3 °C/min from −120 to 180 °C in single cantilever bending mode with sample dimensions of 60 × 6 × 1 mm^3.

The tensile testing was performed on an Instron 1185 (Norwood, Massachusetts) universal tester according to the ISO 527-2 standard at 25 °C. For all samples, the crosshead speed was 50 mm/min, and the average values of five measurements were reported.

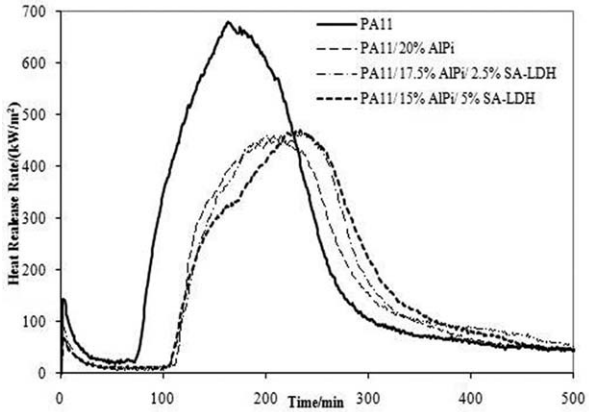

Figure 1. HRR curves of PA11 and its composites.

Table II. Relative Cone Test Data for PA11 and Its Composites

PA11/AlPi/ SA-LDH	pHRR (kW/m^2)	Time to ignition (TTI) (s)	Time to pHRR (T_{pHRR}) (s)	THR (MJ/m^2)	FPI[a] (m^2 s/kW)	FGI[b] (kW/m^2 s)
100/0/0	678.7 ± 17	69 ± 3	161 ± 2	93.2 ± 15	0.1	4.2
80/20/0	459.8 ± 14 (↓32.2%)	107 ± 4 (→38 s)	212 ± 4 (→51 s)	79.4 ± 18 (↓14.8%)	0.23	2.2
80/17.5/2.5	467.4 ± 13 (↓31.1%)	106 ± 4 (→37 s)	230 ± 5 (→69 s)	83.7 ± 19 (↓10.2%)	0.23	2.1
80/15/5	469.7 ± 13 (↓30.8%)	106 ± 5 (→37 s)	234 ± 4 (→73 s)	82.4 ± 16 (↓11.6%)	0.23	2.0

[a] FPI = TTI/pHRR.
[b] FGI = pHRR/T_{pHRR}.

RESULTS AND DISCUSSION

Flame Retardancy

The LOI and UL-94 results of the PA11 composites are shown in Table I. As one can see, the LOI of neat PA11 was about 23.0 and cannot pass any UL-94 rating. The addition of 20% AlPi made the LOI increase to 31.5, at the same time reaching the V-1 rating. Substitution of SA-LDH (2.5–5%) with an equal content of AlPi further lifted the LOI. For the sample with 15% AlPi and 5% SA-LDH added, the LOI reached 32.4.

The cone test results in Figure 1 and Table II illustrate that the addition of 20% AlPi brought a significant improvement in the flame retardancy of PA11. The *peak heat release rate* (pHRR) decreased abruptly from 678.7 kW/m^2 in neat PA11 to 459.4 kW/m^2, a 32.2% drop. Similarly, the *total heat released* (THR) decreased from 93.2 to 79.4 MJ/m^2, a 14.8% drop. At the same time, *time to ignition* (TTI) was prolonged by 38 s, from 69 to 107 s.

There was no obvious change in pHRR and THR values for samples containing SA-LDH, but the HRR curves were shifted to the right, and *time to pHRR* (T_{pHRR}) was prolonged from 161 s in PA11 to 212 s in PA11 with 20% AlPi; for AlPi/SA-LDH additions in the ratios of 17.5%/2.5% and 15%/5%, the T_{pHRR} was further prolonged to 230 and 234 s, respectively. The fire growth index (FGI) is an important parameter in the cone test and is the ratio of pHRR to T_{pHRR} (pHRR/T_{pHRR}) and quantifiably describes the spread rate of fire. The FGI of pristine PA11 was 4.2 kW/m^2 s, which dropped promptly to 2.2, 2.1, and 2.0 kW/m^2 s for AlPi/SA-LDH added in the ratios of 20%/0, 17.5%/2.5%, and 15%/5%, respectively.

The results indicated that heat release during combustion was effectively controlled by AlPi and even further by the AlPi/SA-LDH combination.

The char of the PA11 composites after the cone test was observed by SEM, and the photos are shown in Figure 2. The existence of 20% AlPi made the char so crisp that it can hardly keep as a whole. The 17.5%/2.5% AlPi/SA-LDH combination improved the char quality. The addition of AlPi/SA-LDH at

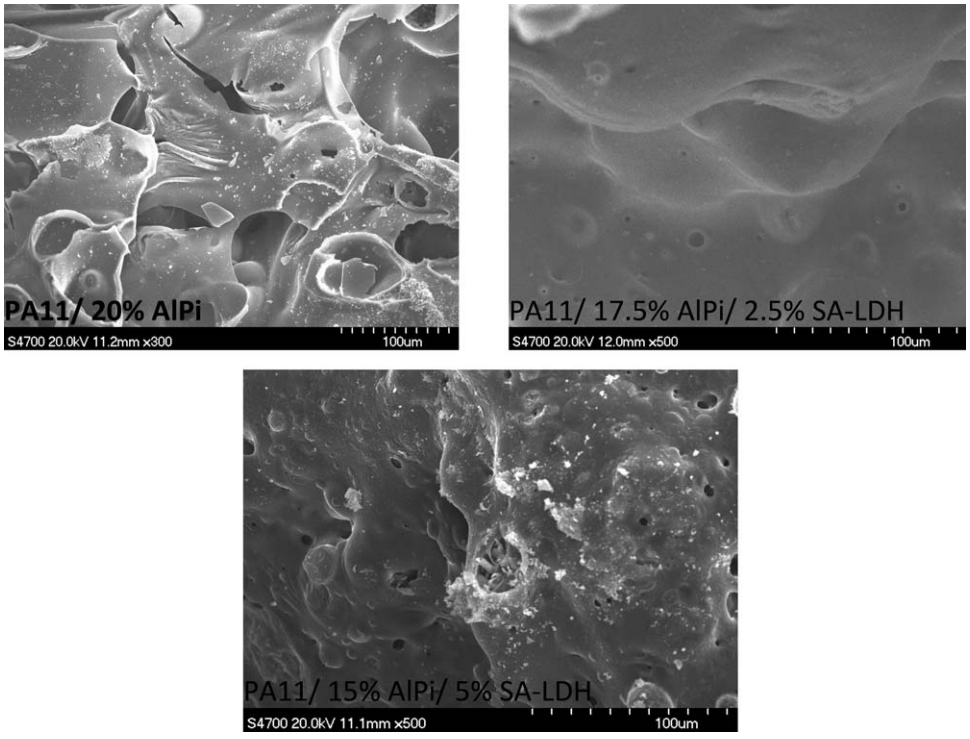

Figure 2. SEM photos of char of PA11 composites.

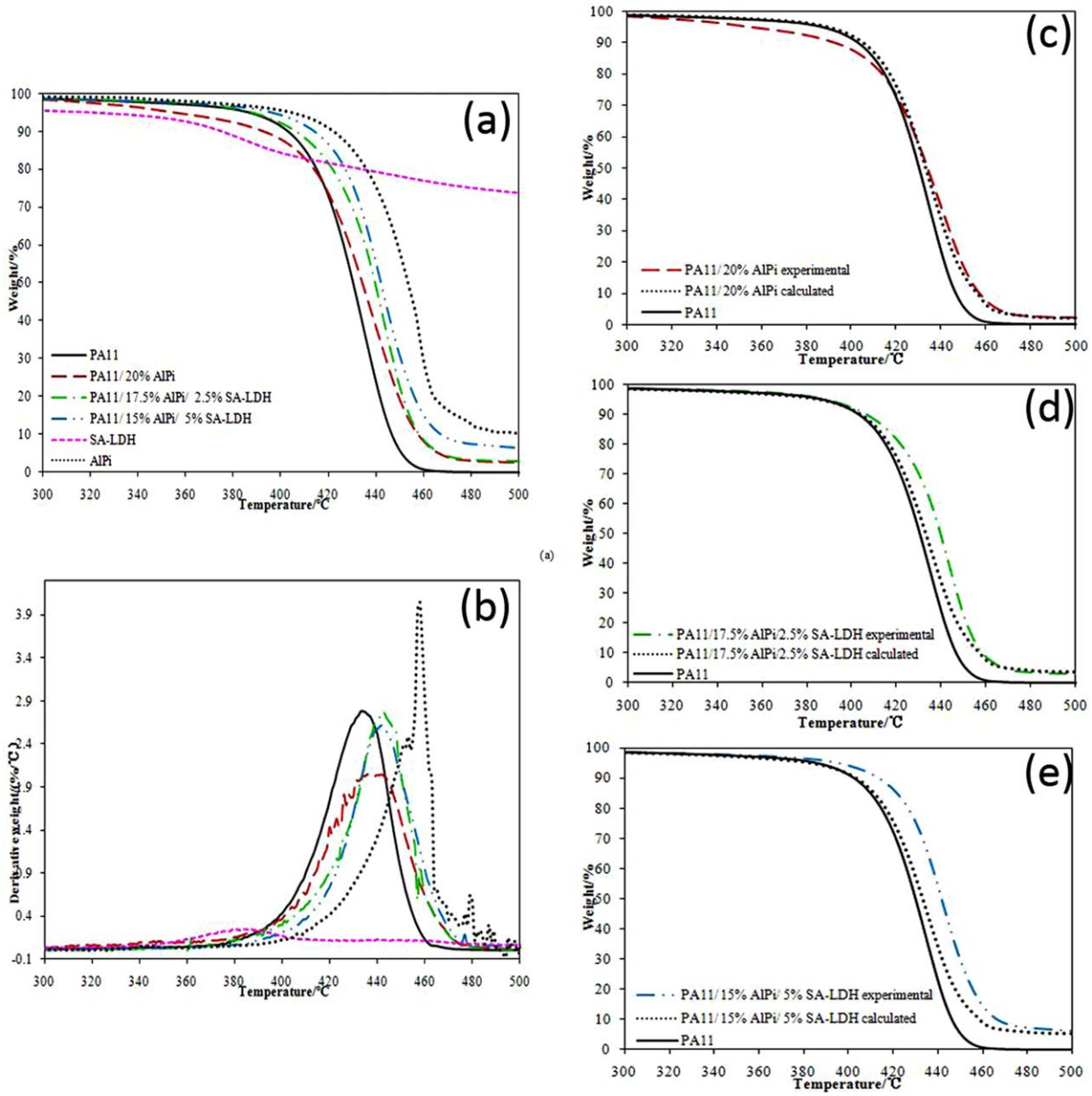

Figure 3. TGA and DTG curves of PA11, AlPi, SA-LDH, and its composites in N_2. [Color figure can be viewed in the online issue, which is available at wileyonlinelibrary.com.]

15%/5% can still keep the char coherent, but small voids can be found. The reason may be that the rigid LDH layers in the composite formed a barrier to protect the material matrix, but with increasing loading of SA-LDH, the water and gas released from SA-LDH decomposition formed small voids in the composite and then destroyed its continuity.

Table III. TGA Results for PA11 and Its Composites

PA11/AlPi/SA-LDH	$T_{10\%}$ (°C)	$T_{50\%}$ (°C), N_2	$m_{char,500\,°C}$	$T_{10\%}$ (°C)	$T_{50\%}$ (°C), Air	$m_{char,650\,°C}$
PA11	403.0	430.3	0.03%	417.3	461.1	4.3%
80/20/0	393.2	434.2	2.4%	375.7	455.4	7.8%
80/17.5/2.5	406.3	439.5	2.9%	421.3	459.3	15.0%
80/15/5	414.1	441.2	6.3%	413.8	459.5	21.2%
AlPi	422.0	453.5	10.4%			
SA-LDH	351.5		72.5%			

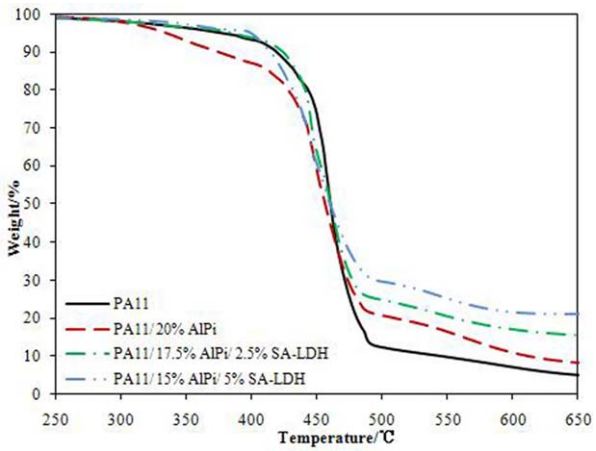

Figure 4. TGA curves of PA11 and its composites in air atmosphere. [Color figure can be viewed in the online issue, which is available at wileyonlinelibrary.com.]

Thermal Stability

The TGA curves in N_2 atmosphere are presented in Figure 3, and relative data are listed in Table III. Figure 3(a) shows that PA11 exhibits a typical one-step degradation, which is generally observed in aliphatic polyamides caused by a depolymerization. The whole weight-loss scope of PA11 was approximately 380–470°C, with 10% ($T_{10\%}$) and 50% weight loss ($T_{50\%}$) occurring at 403 and 430 °C, respectively. Almost no char was left after 500 °C. The decomposition of AlPi happened at a higher temperature in the range 400–480 °C, with $T_{10\%}$ and $T_{50\%}$ occurring at 422 and 454 °C, respectively. However, the initial decomposition of the composite PA11 and 20% AlPi occurred earlier than either PA11 or AlPi, with $T_{10\%}$ occurring at 393 °C. The reaction between PA11 and AlPi resulted in the earlier decomposition of PA11.[8]

The decomposition of SA-LDH was in the range 340–400 °C, much earlier than PA11, but it showed very high char content (72.5% at 500 °C). By 2.5 or 5% SA-LDH substitution with equal AlPi, $T_{10\%}$ and $T_{50\%}$ increased to 406.3, 414.1, and 439.5, 441.2 °C, respectively.

In order to probe the synergism of AlPi/SA-LDH to PA11, more calculations and comparisons were done. Under the assumption of no influence of AlPi and SA-LDH on PA11, the calculated TGA curves of PA11/AlPi/SA-LDH composites according to weight percentage were traced. The calculated and experimental TGA curves are shown in Figure 3(c,d,e). The results illustrate that AlPi/SA-LDH resulted in the TGA curve shifting to the right and the residue increasing, indicating a synergistic effect on thermal stability and char forming.

As shown in Figure 4, the TGA curves in air take the same trend as those in nitrogen in Figure 3. The significant difference was that the char residue content increased to 15.0% (AlPi/SA-LDH = 17.5%/2.5%) and 21.2% (AlPi/SA-LDH = 15%/5%).

The remarkable increase in char content in air can be attributed to at least four reasons. The first one is that water released from the LDH molecule will absorb more heat and then protect PA11 from thermal degradation. At the same time, the decomposition of SA will release nonflammable gas such as NH_3 or SO_2 to dilute the oxygen concentration.[15] The second may be that oxygen in air will react with PA11, AlPi, or SA-LDH to form more char residue. The third is that the earlier-decomposed AlPi will react with oxygen to inhibit further thermal oxidation of PA11.[3] The last one is attributed to the barrier formed by the LDH molecules. Other authors have discussed the improvement of scattered flake nanoparticles such as MMT on the flame retardancy and thermostability of polymer.[20,21]

Thermal Decomposition and Flame-Retardant Mechanism Analysis

The FTIR spectra of raw PA11, SA-LDH, AlPi, and the char of PA11 composites are compared in Figure 5. The characteristic bonds assigned to PA11, such as the N—H stretch at 3300 cm^{-1} and amide I and II at 1635 and 1538 cm^{-1}, disappeared in the char of PA11 composites. However, in AlPi the special peaks at 1245 and 1080 cm^{-1} belonging to the symmetric and asymmetric stretching vibrations of P═O and the peak at 1020 cm^{-1} assigned to P—O[22,23] combined to form a wider peak in the char of PA11/20% AlPi, which means that the basic structure of AlPi was disrupted during heating but some phosphorus compounds remained. Furthermore, the peak around 3600 cm^{-1} assigned to —OH remained in the char of PA11/15% AlPi/5% SA-LDH, meaning that some SA-LDH was still in the char. These results can explain the increase in char content in the TGA test.

In order to reveal the decomposition mechanism, the released gas and residue composition during heating was studied by FTIR-TGA and FTIR synchronously. The FTIR spectra of the residues after calcination in a muffle from 25 to 450 °C are depicted in Figure 6(a), and the FTIR spectra of the volatile products obtained from FTIR-TGA at 450 °C are shown in Figure 6(b).

In the FTIR spectra of either the PA11 residue in a muffle or volatile at 450 °C, characteristic bonds at 2921 and 2852 cm^{-1} assigned to —CH_2 and at 1635 cm^{-1} assigned to —NH_2 can be found, demonstrating that the decomposition mechanism of PA11 is chain scission.

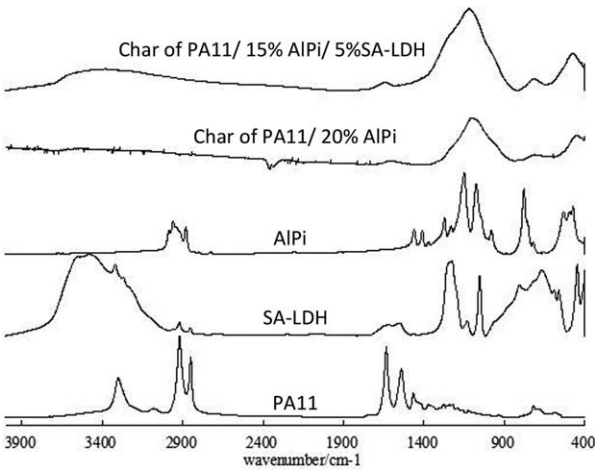

Figure 5. FTIR spectra of raw PA11, SA-LDH, AlPi, and char of PA11 composites.

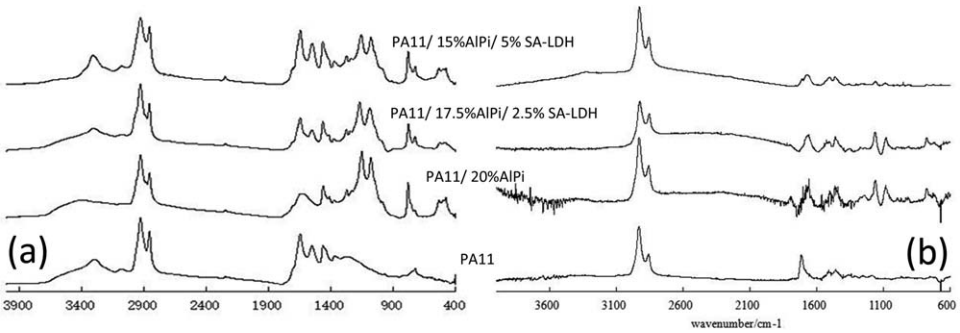

Figure 6. FTIR spectra of thermolysis product of PA11 and its composites at 450 °C: (a) residue after calcination in muffle; (b) volatile product from TGA-FTIR.

In the FTIR spectra of PA11/20% AlPi at 450 °C, all characteristic bonds belonging to PA11 (2921, 2852, and 1635 cm^{-1}) and AlPi (1245, 1080, and 1020 cm^{-1}) can be found in either residue or volatile, indicating the simultaneous decomposition of PA11 and AlPi at relatively high temperature.

In contrast, in the FTIR spectra of PA11/15% AlPi/5% SA-LDH at 450 °C, all of the characteristic bonds belonging to PA11 (2921, 2852, and 1635 cm^{-1}) and AlPi (1245, 1080, and 1020 cm^{-1}) changed a little. The intensity fades down in the spectra of volatiles, which means in the presence of SA-LDH the decomposition of AlPi was hindered, and PA11 was protected eventually.

It is generally considered that the flame-retardant contribution from organophosphorous products is coming from the condensed phase.[24] Phosphoric acid and polyphosphates generated during heating will form a viscous char layer on the surface of the polymer matrix. With the coexistence of both phosphorus and nitrous oxide, a pasty char containing P—N—P and P—C will form and cover the polymer to inhibit further combustion.

However, a gas-phase flame-retardant contribution was exhibited by SA. An incombustible gas including NH_3, N_2, SO_2, and vapor released during heating will dilute the O_2 concentration and absorb combustion heat.

Flaky LDH molecules will form a barrier to isolate the polymer from heat and combustion. In summary, the synergistic flame retardancy of AlPi and SA-LDH is shown in Scheme 1.

Mechanical Properties

The influence of AlPi and SA-LDH on the mechanical performance of PA11 is shown in Figure 7.

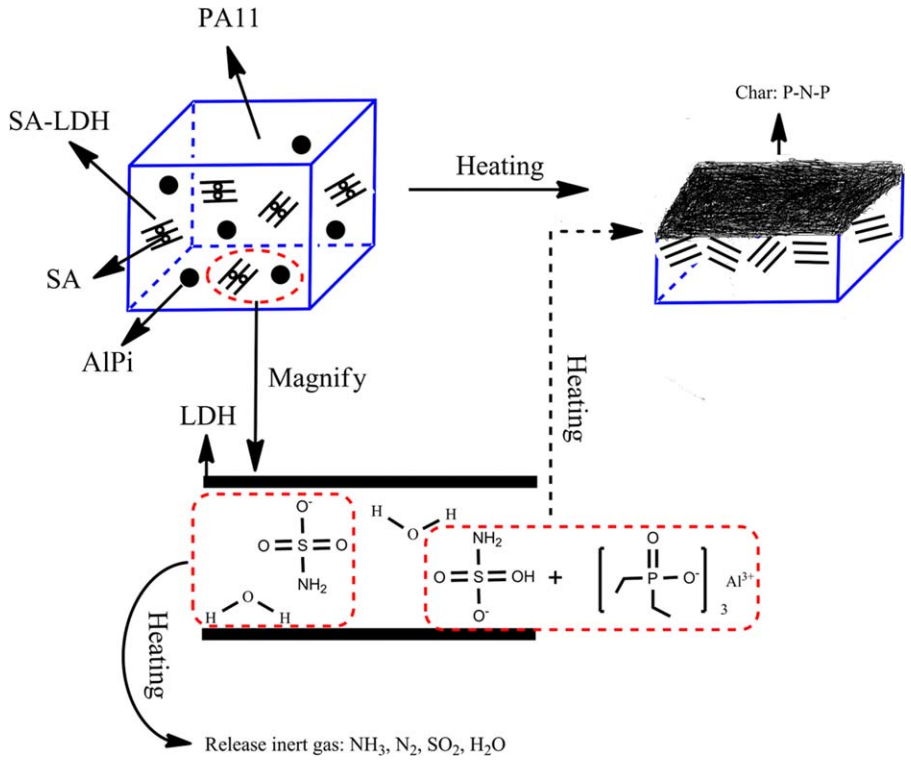

Scheme 1. Synergistic flame retardant of AlPi and SA-LDH to PA11. [Color figure can be viewed in the online issue, which is available at wileyonlinelibrary.com.]

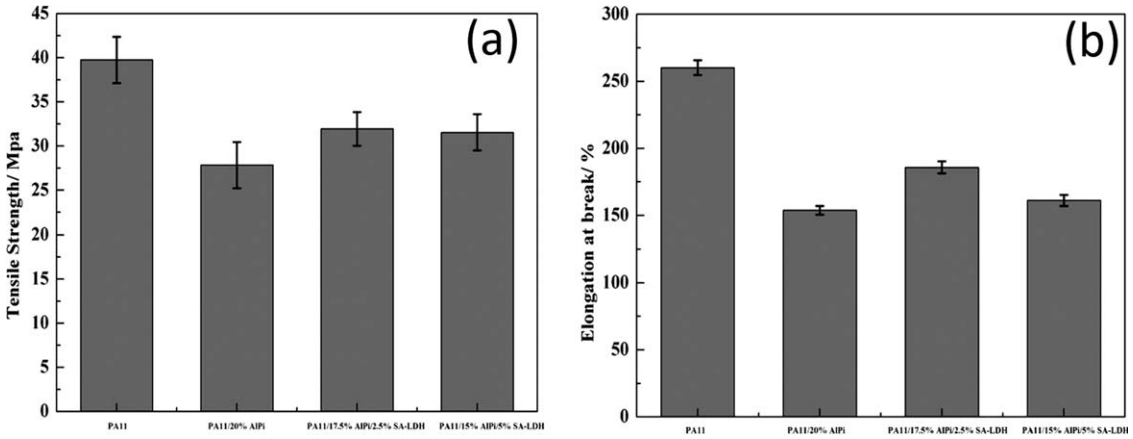

Figure 7. (a) Tensile strength and (b) elongation at break of PA11 and its composites.

In general, the introduction of a flame retardant will create an unavoidable deterioration in the mechanical performance of composites.[25] A similar trend occurred in the PA11/AlPi system. The addition of 20% AlPi resulted in an obvious decrease in both tensile strength (a 28.6% drop) and elongation at break (a 40.9% drop). The trend was restrained after the substitution of SA-LDH with an equal dosage of AlPi. The introduction of SA-LDH not only brought an improvement in flame retardancy but also inhibited the worsening of mechanical performance.

The influence of AlPi and SA-LDH on the evolution of the storage modulus (E') with temperature is shown in Figure 8(a). It can be seen that the E' of PA11 decreased after the introduction of AlPi and SA-LDH. The addition of 20% AlPi brought about a 450 MPa drop in E' before the glass transition; however, with 5% SA-LDH substitution with equal dosage of AlPi, there was only a 150 MPa drop in E' before the glass transition. But after 50 °C, little difference can be found for either 20% AlPi or AlPi/SA-LDH (15%/5%) additions, which means the reinforcement by SA-LDH was just exhibited below the T_g. The possible reason

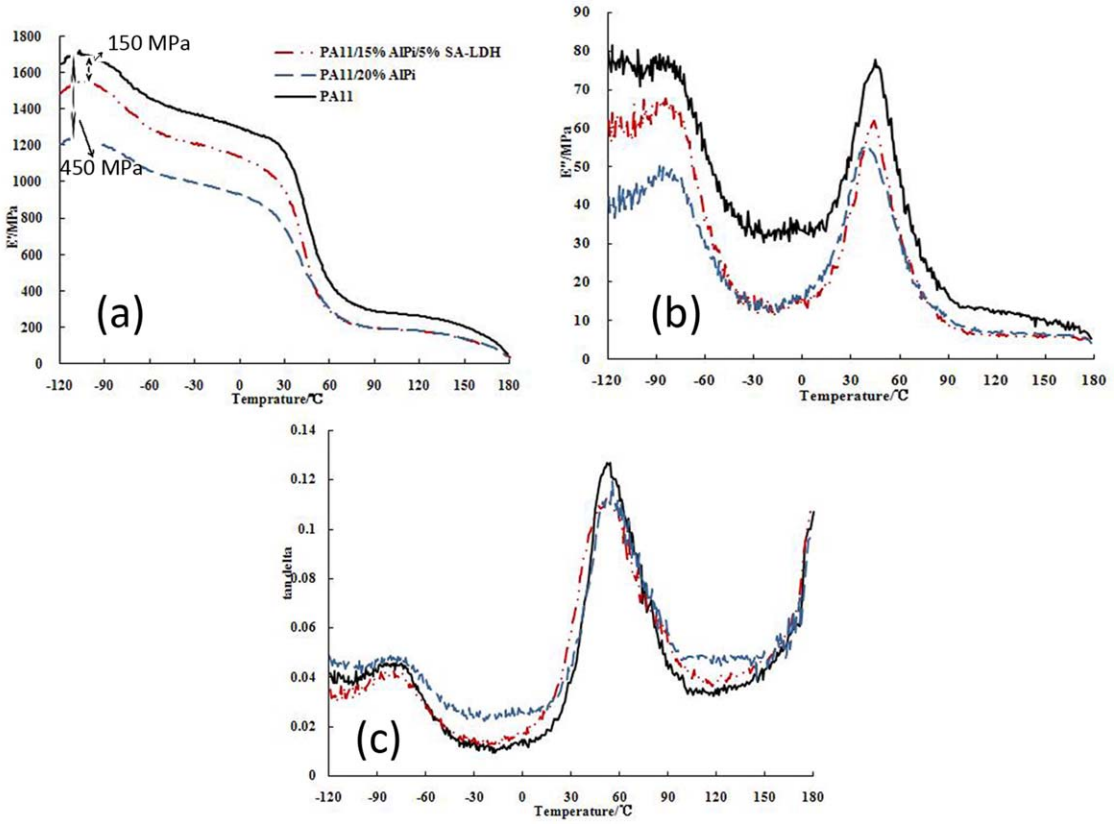

Figure 8. DMA curves of PA11 and its composites: (a) storage modulus (E'); (b) loss modulus (E''); (c) tan δ. [Color figure can be viewed in the online issue, which is available at wileyonlinelibrary.com.]

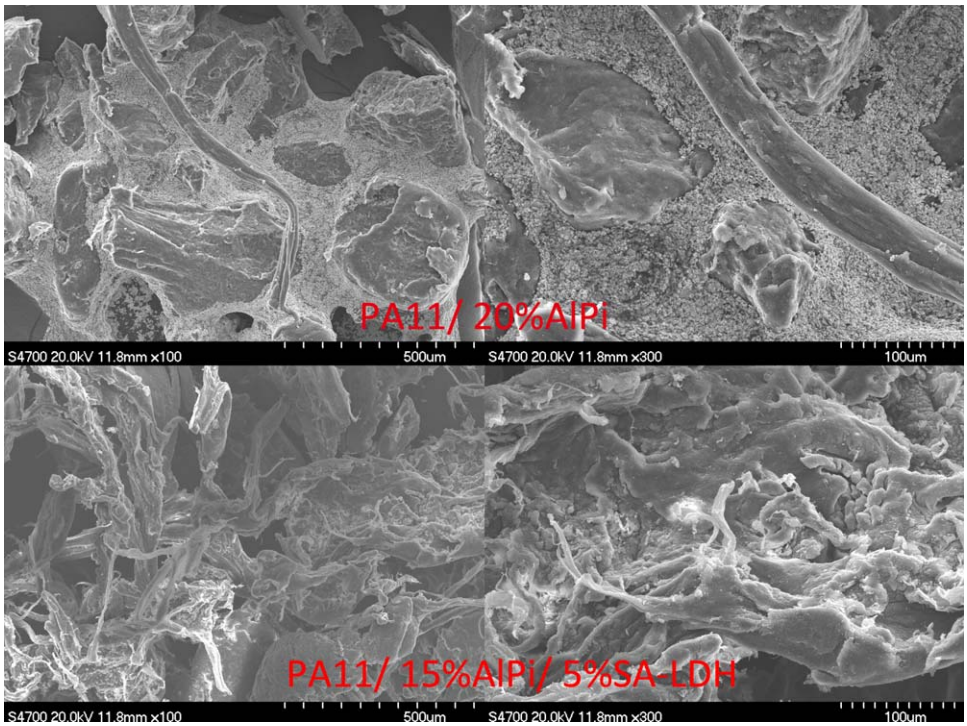

Figure 9. SEM photos of PA11 composites. [Color figure can be viewed in the online issue, which is available at wileyonlinelibrary.com.]

may be that SA-LDH dominantly acts on the crystal phase as a heterogeneous nucleating agent. SA-LDH induced the formation of the α form, which exhibits a higher modulus below T_g but a more rapid decrease with temperature above T_g.[26,27]

The evolution of the loss modulus (E'') with temperature is shown in Figure 8(b). The maximum E'' in pristine PA11 means the best flexibility of the polymer chains deteriorated after the introduction of inorganic particles such as AlPi or SA-LDH. The greatest drop in E'' appeared in 20% AlPi, which means AlPi had more influence on the molecular chain motion during the glass transition.

Figure 8(c) shows the loss factor (tan δ) versus temperature curves, and in each curve two relaxation peaks can be found, the smaller one in the range −100 to −60 °C describing the relaxation of unbounded small groups involving —NH_2 and —CH_2 in the amorphous phase.[28] For the relatively low portion of these groups, the influence of additives was not considerable. However, the bigger peak emerging from 30 to 80 °C was relevant to the glass transition, corresponding to the long-range macromolecular mobility. The area of this peak means the flexibility of the polymer matrix. The maximum area for pristine PA11 means the best flexibility compared with samples incorporating AlPi and SA-LDH. And the minimum area emerging in 20% AlPi illustrates that AlPi acts mainly on the amorphous phase and influences the motion of molecular chains during the glass transition.

Mechanism Analysis on the Mechanical Performance

The strengthening effect caused by SA-LDH was further explored. The phase separation is so clear in the SEM photos shown in Figure 9 of PA11/20% AlPi with the distributed size of AlPi at about 100 to 200 μm; however, at the same magnification, phase separation in PA11/15% AlPi/5% SA-LDH was not obvious. The SEM observation indicated that SA-LDH acted as a compatibilizer and improved the miscibility of PA11 and AlPi. The interaction among PA11, AlPi, and SA-LDH was studied by XPS.

At first, it was easily found from the XPS spectra in Figure 10 that, compared with SA-LDH, the S_{2P} peak was widened and shifted a little to the right in PA11/15% AlPi/5% SA-LDH. Because the element S only existed in SA-LDH, the change illustrated that some molecular interaction between SA-LDH and PA11 or AlPi really existed. Based on the molecular structure shown in Scheme 2, it is reasonable to form a H bond between amino (N—H) and hydroxy (H—O) in SA-LDH, which is possible to be disrupted in the ternary system of PA11, SA-LDH, and AlPi, for new intermolecular action to be formed.

Similarly, element P only existed in AlPi. As shown in Figure 9, the peak situation and width of P_{2P} showed little difference in AlPi and PA11/20% AlPi, which means there is almost no intermolecular force between AlPi and PA11 in their composites, but in PA11/15% AlPi/5% SA-LDH, the peak was widened and shifted a little to the left to lower binding energy, which should be caused by the interaction between AlPi and SA-LDH. In any case, it is reasonable to form a H bond between N—H in SA-LDH and P═O in AlPi.

Analogously, the little difference in AlPi and PA11/20% AlPi in the N_{1S} spectra also documented a rare interaction between

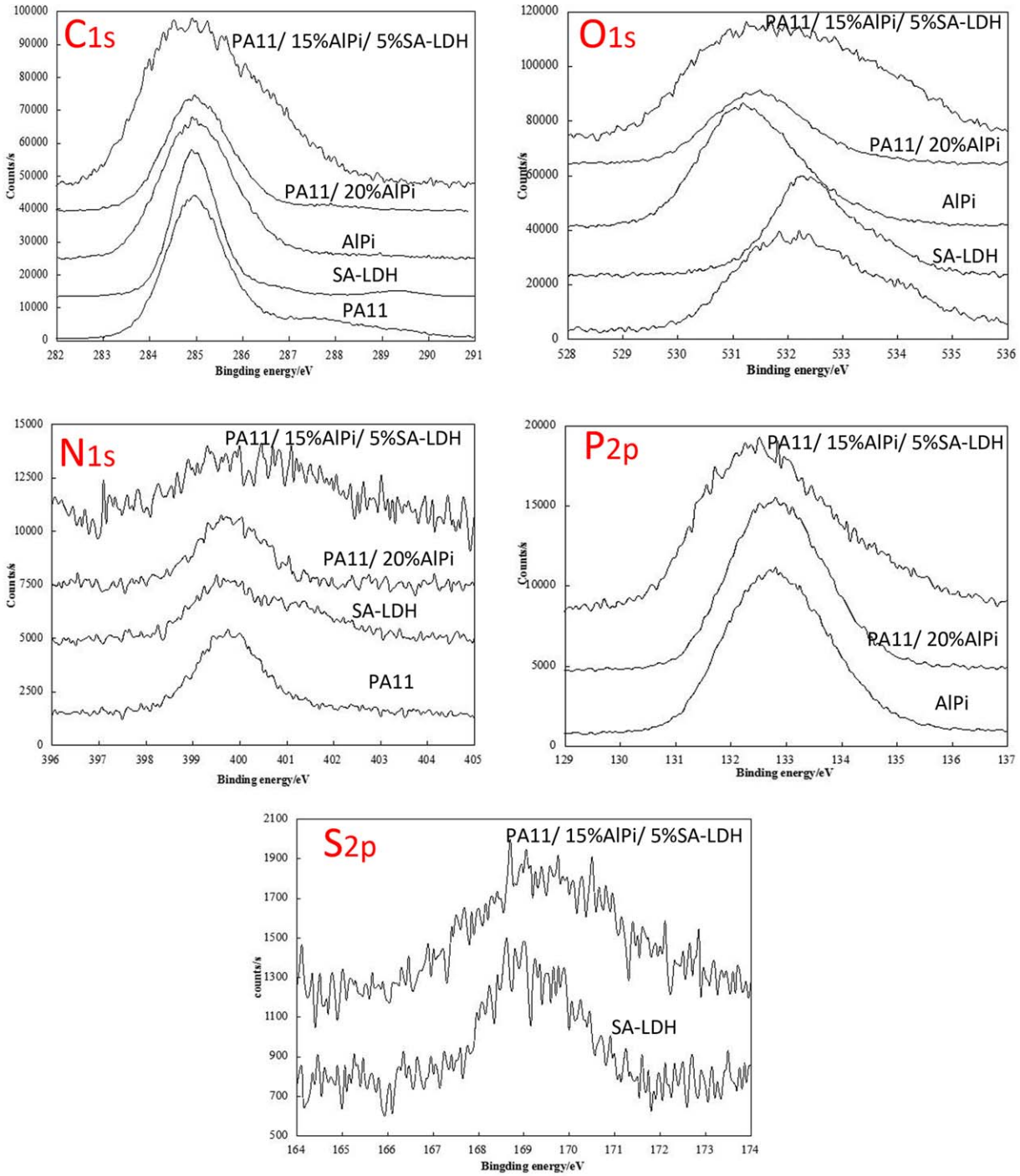

Figure 10. XPS spectra of PA11, SA-LDH, AlPi, and PA11 composites. [Color figure can be viewed in the online issue, which is available at wileyonlinelibrary.com.]

AlPi and PA11. It is also well known that the intra- and intermolecular H bonds between amino (N—H) and carbonyl (C═O) is ubiquitous in PA materials, as shown in Scheme 2. The width and situation of the N_{1S} peaks in SA-LDH and PA11 both changed in PA11/15% AlPi/5% SA-LDH, which means that the H bonds stemming from the amino of SA-LDH and the PA11 inside were both disrupted, and new bonds were formed in the ternary system.

Because C and O exist in SA-LDH, AlPi, and PA11, it is difficult to analyze the binding mode among them. In any case, the widened C_{1S} and O_{1S} peaks in PA11/15% AlPi/5% SA-LDH evidenced the interaction in the ternary system.

In summary, SA-LDH could interact with both PA11 and AlPi. In other words, SA-LDH acted as a compatibilizer to improve the miscibility of PA11 and AlPi, which has been assumed by

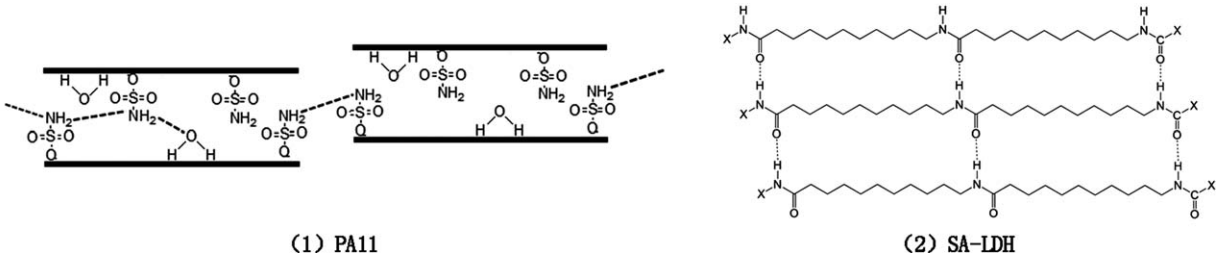

Scheme 2. Intra- and intermolecular H bond in (1) PA11 and (2) SA-LDH.

SEM observation. In the ternary system, new intermolecular H bonds among SA-LDH, AlPi, and PA11 were formed, and as a result the binding situation of the elements changed.

CONCLUSIONS

Sulfamic acid–intercalated LDH (SA-LDH) was prepared and melted with AlPi together into PA11. The characterization results showed that AlPi/SA-LDH combination was more effective than AlPi on improving the flame retardancy and thermostability of PA11 at the same loading. The thermal decomposition and flame-retardant mechanisms were revealed by analysis of the group constitution of residues and volatile gas during heating. With the existence of SA-LDH, the decomposition of AlPi and PA11 were both prolonged. The deterioration in mechanical performance caused by AlPi was partly improved by SA-LDH introduction, reflected in the tensile strength, elongation, and modulus. Incorporation of SA-LDH improved the mechanical performance by promoting miscibility between PA11 and AlPi.

ACKNOWLEDGMENTS

The authors would like to thank the National Natural Science Foundation of China (No. 51373018 and 21374004) and Fundamental Research Funds for the Central Universities (YS201402) for their financial support.

REFERENCES

1. Jimenez, M.; Gallou, H.; Duquesne, S.; Jama, C.; Bourbigot, S.; Couillens, X. *J. Fire Sci.* **2012**, *30*, 535.
2. Stoclet, G.; Segue La, R. S.; Lefebvre, J. M. *Polymer* **2011**, *52*, 1417.
3. Zhan, Z. S.; Xu, M. J.; Li, B. *Polym. Degrad. Stab.* **2015**, *117*, 66.
4. Schmitt, E. *Plast. Addit. Compd.* **2007**, *9*, 26.
5. Bourbigot, S.; Duquesne, S.; Fontainea, G.; Bellayera, S.; Turfa, T.; Samya, F. *Mol. Cryst. Liq. Cryst.* **2008**, *486*, 325.
6. Samya, F.; Bourbigot, S.; Jama, C.; Bellayer, S.; Nazare, S.; Hull, R.; Fina, A.; Castrovinci, A.; Camino, G. *Eur. Polym. J.* **2008**, *44*, 1631.
7. Lao, S. C.; Koo, J. H.; Moon, T. J. *J. Fire Sci.* **2011**, *29*, 479.
8. Samya, F.; Bourbigot, S. *Polym. Degrad. Stab.* **2012**, *97*, 2217.
9. Naik, A. D.; Fontainea, G.; Samyna, F.; Delvab, X.; Bourgeoisb, Y.; Bourbigot, S. *Polym. Degrad. Stab.* **2013**, *98*, 2653.
10. Leng, J.; Purohit, P. J.; Kang, N. J.; Wang, D. Y. *Eur. Polym. J.* **2015**, *68*, 338.
11. Lennerová, D.; Kovanda, F.; Brožek, J. *Appl. Clay Sci.* **2015**, *114*, 265.
12. Abdallah, W.; Yilmazer, U. *J. Appl. Polym. Sci.* **2013**, *127*, 772.
13. Mehmet, D.; Erdal, B. *Fire Mater.* **2014**, *38*, 92.
14. Horacek, H.; Grabner, R. *Polym. Degrad. Stab.* **1996**, *54*, 205.
15. Liu, X. S.; Gu, X. Y.; Zhang, S. *J. Appl. Polym. Sci.* **2013**, *130*, 3645.
16. Jiang, Y.; Gu, X. Y.; Zhang, S.; Tang, W. F. *Mater. Lett.* **2015**, *150*, 31.
17. Coquelle, M.; Duquesne, S.; Casetta, M.; Sun, J.; Zhang, S.; Bourbigot, S. *Polym. Degrad. Stab.* **2014**, *106*, 150.
18. Lewin, M.; Zhang, J.; Pearce, E.; Gilman, J. *Polym. Adv. Technol.* **2007**, *18*, 737.
19. Lewin, M. *Polym. Degrad. Stab.* **2011**, *96*, 256.
20. Kiliaris, P.; Papaspyrides, C. D. *Prog. Polym. Sci.* **2010**, *35*, 902.
21. Dasari, A.; Yu, Z. Z.; Cai, G. P.; Mai, W. *Prog. Polym. Sci.* **2013**, *38*, 1357.
22. Wu, Q. J.; Liu, X. H.; Lars, A. B. *Polymer* **2002**, *43*, 2445.
23. Triantafillidis, C. S.; LeBaron, P. C.; Pinnavaia, T. *J. Chem. Mater.* **2002**, *14*, 4088.
24. Ye, L.; Qu, B. *J. Polym. Degrad. Stab.* **2008**, 93, 918.
25. Laoutid, F.; Bonnaud, L.; Alexandre, M.; Lopez-Cuesta, J. M.; Dubois, P. *Mater. Sci. Eng., R* **2009**, *63*, 100.
26. Liu, X. H.; Wu, Q. J. *Eur. Polym. J.* **2002**, *38*, 1383.
27. Liu, T. X.; Liu, Z. H.; Ma, K. X. *Compos. Sci. Technol.* **2003**, *63*, 331.
28. Nyambo, C.; Kandare, E.; Wilkie, C. A. *Polym. Degrad. Stab.* **2009**, *94*, 513.